Electronic Supplementary Material (ESI) for Chemical Communications

Supporting information

Mapping local electric fields in proteins at biomimetic interfaces

Gal Schkolnik[1], Tillmann Utesch[1], Johannes Salewski[1], Katalin Tenger[2], Diego Millo[1], Anja Kranich[1], Ingo Zebger[1], Claudia Schulz[1], László Zimányi[2], Gábor Rákhely[3], Maria Andrea Mroginski[1], Peter Hildebrandt[1*]

[1] Technische Universität Berlin, Institut für Chemie, Sekr. PC14, Straße des 17. Juni 135, D-10623 Berlin, Germany;

[2] Institute of Biophysics, Biological Research Centre, H-6726 Szeged Temesvári krt. 62., Hungary;

[3] Department of Biotechnology, University of Szeged, Közép fasor 52, H-6726 Szeged, Hungary

* Corresponding author. Email: hildebrandt@chem.tu-berlin.de

Content:

1. Preparation of labelled proteins

Cyt-*c* mutants were produced by site-directed mutagenesis and purified, according to procedures previously described by Tenger et al.[1,2]. The plasmids containing the mutated genes for the expression of the K8C and K39C mutant cytochromes *c* have been verified by sequencing. The final purity of the protein was reached by chromatography on a CM-Sephadex C50 cation exchange matrix. The purity was checked by UV-visible spectroscopy as well as SDS-gel electrophoresis (Fig. S0).

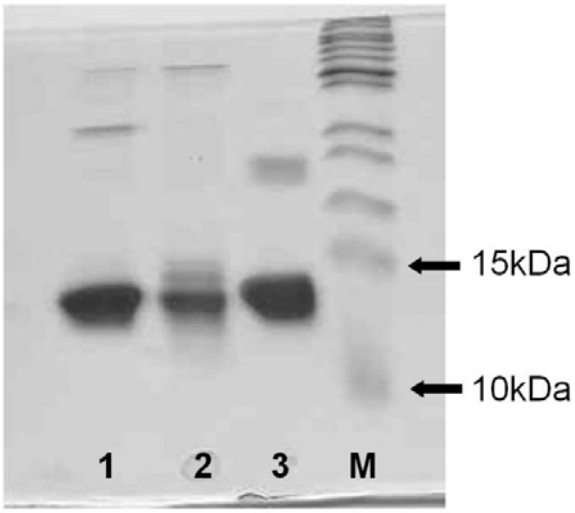

Figure S0. SDS-gel electrophoresis of horse heart cytochrome *c* variants. Lane 1 and 2: heterologously expressed, purified K8C and K39C mutants, respectively. Lane 3: Wild type. Lane M: protein ladder (Fermentas SM0671).

The protein variants were labelled with a Stark shift sensitive 4-mercaptobenzonitrile (MBN). MBN was covalently bound to the cysteine residue at the mutation site, as follows: The protein, at a concentration of 50 µM in 75 mM sodium-phosphate buffer, pH 7.0, was mixed with a 100-fold molar excess of MBN (Apin chemicals, Milton Park, UK) solvated in dimethylsulfoxide (DMSO). The mixture was stirred overnight at 4°C. Centrifugation at 5000 g was used to separate the protein-containing supernatant from MBN precipitate. The supernatant was then dialyzed against a phosphate buffer, in order to remove any residual unbound label. The purity, structural, and functional integrity of the labelled proteins was checked by UV-vis absorption spectroscopy, cyclic voltammetry, and SEIRA redox titration (see below Figure S2).

Sequence of Horse heart Cyt-c (according to pdb 1Akk)

1	GLY	ASP	VAL	GLU	LYS	GLY	LYS	**LYS**	ILE	PHE
11	VAL	GLN	LYS	CYS	ALA	GLN	CYS	**HIS**	THR	VAL
21	GLU	LYS	GLY	GLY	LYS	HIS	LYS	THR	GLY	PRO
31	ASN	LEU	HIS	GLY	LEU	PHE	GLY	ARG	**LYS**	THR
41	GLY	GLN	ALA	PRO	GLY	PHE	THR	TYR	THR	ASP
51	ALA	ASN	LYS	ASN	LYS	GLY	ILE	THR	TRP	LYS
61	GLU	GLU	THR	LEU	MET	GLU	TYR	LEU	GLU	ASN
71	PRO	LYS	LYS	TYR	ILE	PRO	GLY	THR	LYS	**MET**
81	ILE	PHE	ALA	GLY	ILE	LYS	LYS	LYS	THR	GLU
91	ARG	GLU	ASP	LEU	ILE	ALA	TYR	LEU	LYS	LYS
101	ALA	THR	ASN	GLU						

red: lysine residues that were mutated; yellow: Cys residues that covalently bind the heme; blue: axial ligands of the heme

Chemicals. 6-Mercaptohexanoic acid (C5), Dojindo, was used without further purification. The water used in all experiments was purified by a Millipore system and its resistance was greater than 18 MΩ. Di-potassium hydrogen phosphate (K_2HPO_4, ≥ 99%) and potassium di-hydrogen phosphate (KH_2PO_4, ≥ 99%) were purchased from Merck.

2. Vibrational spectroscopy

2.1 IR transmission measurements

IR transmission spectra were recorded with a spectral resolution of 4 cm^{-1} using a Bruker Tensor 27 spectrometer, equipped with a liquid nitrogen-cooled photoconductive MCT detector. The sample compartment was purged with dried air. The sample was held in a temperature-controlled (10°C) gas-tight IR cell for liquid samples (volume ~ 7 µL, path length = 50 µm), equipped with CaF_2 windows. 20,000 scans were accumulated for each spectrum.

2.2 SEIRA measurements

SEIRA measurements were performed using a Kretschmann-ATR configuration using a hemi-

cylindrical shaped silicone (Si) crystal (20 × 25 × 10 mm of W × L × H) under an angle of incidence of 60°. Thin, nano-structured gold (Au) films were formed on the polished surface of the Si substrate by electroless (chemical) deposition.[3] The formation of SAMs followed a protocol previously described.[4] For the immobilization of both Cyt-c variants, the 6-mercaptohexanoic acid SAM coated gold film was immersed in a 2 μM Cyt-c solution. SEIRA spectra were recorded at a range from 4000 to 1000 cm^{-1}, with a spectral resolution of 4 cm^{-1} on a Bruker IFS66v/s spectrometer equipped with a photoconductive MCT detector. 400 scans were co-added for each spectrum; three to five spectra were recorded for each experiment and averaged. A representative SEIRA spectrum is shown in Fig. S1.

For SEIRA measurements at an applied potential (Fig. S2), the ATR crystal was incorporated in a three-electrode home-built cell, constructed based on a previously published design.[5] The Au-film on the ATR crystal, a Pt wire, and a Ag/AgCl (3 M KCl) electrode served as working, counter, and reference electrode, respectively. Electrode potentials were controlled by an Autolab PGSTAT 12 potentiostat.[6]

IR transmission experiments were repeated twice, and SEIRA experiments 3-4 times, for each Cyt-c variant. Average values are reported. The corresponding standard deviation for IR transmission measurements is 0.15 cm^{-1} for both mutants, and for SEIRA 0.4 cm^{-1} for K39C and 0.9 cm^{-1} for K8C. All measurements were performed at 10° C, in a 10 mM potassium phosphate buffer, corresponding to an ionic strength of 22 mM, at pH 7.0. Accordingly, the reciprocal Debye length is calculated to be $5x10^{8}$ m^{-1}.

For both variants, in the SEIRA experiments the vibrational stretching band of the CN label slowly disappears upon attachment of the protein to the SAM, notably at a rate ca. 5 times faster for the K8C compared to the K39C variant. We attribute this effect to the cleavage of the bound label by reactive oxygen species generated in the electrode/electrolyte interface. This unwanted side reaction would require only traces of oxygen, which could not be avoided within the present experimental setup.

2.3. Data analysis

IR and SEIRA spectra were either analysed using the second derivative or by fits of Gaussian functions to the spectra after background subtraction. Both approaches yield identical results. Note that there are variations in the shape of the peak indicating a (asymmetric) broadening. Thus, satisfactory fits required in some cases additional Gaussian functions albeit with weak amplitudes. For the analysis, only the main peak frequency was considered. As a consequence of these changes from experiment to experiment, the variation of the nitrile stretching frequency determined form the IR and SEIRA spectra was ±0.15 for the IR, ±0.4 for K39C SEIRA and ±0.9 for K8C SEIRA measurements. Non-covalently bound MBN displays a band at a frequency (ca. 2225 cm^{-1}, attributed to solid MBN, see Figure S3 for a Raman spectrum of solid MBN.) that is distinctly lower than that of the covalently bound label. The solid MBN occurs due to precipitation of this rather water-insoluble compound, and the corresponding band disappears upon repeated centrifugation and dialysis. Thus, the purity of the labelled protein can readily be checked on the basis of the IR spectra.

2.4. Raman spectroscopy

Raman spectra of MBN were obtained with 1064-nm excitation using an RFS-Raman spectrometer (Bruker Optics). The laser power at the sample was 80 mW and the resolution 4 cm^{-1}; the accumulation time was ca. 1 h (Fig. S3).

3. Electrochemical measurements

Cyclic voltammograms of the labelled K39C and K8C variants were carried out as described previously[6] (Fig. S2).

4. MD Simulations

4.1. Preparation of Cytochrome *c* mutants

All calculations have been based on the minimized NMR structure of reduced horse-heart cytochrome *c* (PDB accession code 2FRC).[7] Two single mutations of Lys-8 and Lys-39 to cysteine, labelled with MBN, were incorporated into the structure with the CHARMM package.[8] These modified structures are denoted as MBN-labelled K8C and MBN-labelled K39C. In order to be consistent with the CHARMM22 force field,[9] we have used the CHARMM partial charges of phenylalanine for the benzene ring, the disulfide patch for the disulfides and the standard amino acid backbone for the backbone. The nitrile charges were derived by density functional theory (B3LYB/6-31g(d)) calculations of MBN, employing the GAUSSIAN 09.[10] The charges of the benzene ring carbons linked to the nitrile and sulfur were adjusted manually, in order to maintain charge neutrality for the label (Table S1). The modified protein structures were protonated according to pH 7 with the CHARMM package.[8] The histidine residues were protonated on the N_δ atoms unless the environment suggested another configuration. The heme cofactor (taken to be reduced) was simulated with the CHARMM parameter set.[9] For both protein variants, the charge was +7e.

4.2. Preparation of the SAM and surface systems

For the self-assembled monolayer (SAM) of 6-mercaptohexanoic acid, the CHARMM force field of lipids[11] was used, but the SAM sulfur atoms and the gold layer were handled as uncharged fixed bodies in order to maintain the separation of 4.96 Å between the sulfur atoms.[12] The protonation level of the carboxyl head-groups was set to 92%, which resulted in a total charge of -30 e for the surface. The initial orientation of the mutants on the surface was chosen according to the protein dipole moment calculated with VMD 1.8.7.[13] These settings assume a strong electrostatically driven adsorption of cytochrome *c* on the SAM. In the initial structure, the separation distance between the mutants and the SAM was set to 5 Å.

4.3. Molecular dynamics (MD) simulations

MD simulations of the MBN-labelled K8C and MBN-labelled K39C mutants in solution and on the SAM covered gold surface were performed with NAMD 2.6[14] using the CHARMM22 force-field.[9] The systems were solvated with TIP3 water[15] and Na^+ and Cl^- ions were inserted with the VMD 1.8.7 package[13] to gain a neutrally charged system with an ionic strength of ~50 mM, close to the value used in experiments. The systems of more than 42,000 atoms were minimized and heated to 300 K. Following an equilibration of 100 ps, we performed 10 ns long NVT Langevin piston dynamics with a time-step of 2 fs enabled by rigid bonds to all hydrogens.[16] The simulations were carried out under periodic boundary conditions with a simple cut-off of 12 Å for vdW interactions and the particle-mesh Ewald (PME) summation for long-range electrostatics.[17] According to energy and rmsd analysis, the whole system and the protein kept stable during all simulations (Figs. S4 and S5). During the last 5 ns of simulations of Cytochrome *c* mutants on the surface, where the protein is equilibrated (Fig. S5), minimal distances between the CN label and the gold slab and angles between the heme plane and the surface normal or the CN label were averaged (Table S1, Figs. S6 and S7).

The MD simulations indicate that the nitrile label is solvent exposed in both variants as illustrated in Fig. S8.

References

1. Tenger, K.; Khoroshyy, P.; Kovács, K. L.; Zimányi, L.; Rákhely, G.; *Acta Biol. Hung.* **2007,** *58* (Suppl.), 23–35.
2. Tenger, K.; Khoroshyy, P.; Rákhely, G.; Zimányi, L.; *J Bioenerg. Biomembr.* **2010,** *42*,125–133.
3. Miyake, H.; Ye, S.; Osawa, M. *Electrochemistry Communications* **2002,** *4(12)*, 973–977.
4. Murgida, D.H.; Hildebrandt, P. *J. Phys. Chem. B* **2001,** *105*, 1578–1586.
5. Ataka, K.; Heberle, J. *Anal. Bioanal. Chem*. **2007,** 388, 47–54.
6. Wisitruangsakul, N.; Zebger, I.; Ly, K.H.; Murgida, D.H.; Egkasit, S.; Hildebrandt, P. *Phys. Chem. Chem. Phys.* **2008,** *10*, 5276–5286.
7. Xiurong Qi, P.; Beckman, R.A.; Wand, A.J. *Biochemistry* **1996,** *35,* 12275–12286.

8. Brooks, B.R.; Bruccoleri, R.E.; Olafson, B.D.; States, D.J.; Swaminathan, S.; Karplus, M. *J. Comput. Chem.* **1983,** *4(2)*,187–217.
9. MacKerell, Jr., A. D.; Bashford, D.; Bellott, M.; Dunbrack, Jr., R. L.; Evanseck, J. D.; Field, M. J.; Fischer, S.; Gao, J.; Guo, H.; Ha, S.; Joseph-McCarthy, D.; Kuchnir, L.; Kuczera, K.; Lau, F. T. K.; Mattos, C.; Michnick, S.; Ngo, T.; Nguyen, D. T.; Prodhom, B.; Reiher, III, W. E.; Roux, B.; Schlenkrich, M.; Smith, J. C.; Stote, R.; Straub, J.; Watanabe, M.; Wio´rkiewicz-Kuczera, J.; Yin, D.; Karplus, M. *J. Phys. Chem. B* **1998**, *102*, 3586–3616.
10. Frisch, M.J.; Trucks, G.W.; Schlegel, H.B.; Scuseria, G.E.; Robb, M.A.; Cheeseman, J.R.; Scalmani, G.; Barone, V.; Mennucci, B.; Petersson, G.A.; Nakatsuji, H.; Caricato, M.; Li, X.; Hratchian, H.P.; Izmaylov, A.F.; Bloino, J.; Zheng, G.; Sonnenberg, J.L.; Hada, M.; Ehara, M.; Toyota, K.; Fukuda, R.; Hasegawa, J.; Ishida, M.; Nakajima, T.; Honda, Y.; Kitao, O.; Nakai, H.; Vreven, T.; Montgomery, Jr., J.A.; Peralta, J.E.; Ogliaro, F.; Bearpark, M.; Heyd, J.J.; Brothers, E.; Kudin, K.N.; Staroverov, V.N.; Kobayashi, R.; Normand, J.; Raghavachari, K.; Rendell, A.; Burant, J.C.; Iyengar, S.S.; Tomasi, J.; Cossi, M.; Rega, N.; Millam, J. M.; Klene, M.; Knox, J.E.; Cross, J.B.; Bakken, V.; Adamo, C.; Jaramillo, J.; Gomperts, R.; Stratmann, R.E.; Yazyev, O.; Austin, A.J.; Cammi, R.; Pomelli, C.; Ochterski, J.W.; Martin, R.L.; Morokuma, K.; Zakrzewski, V.G.; Voth, G.A;. Salvador, P.; Dannenberg, J.J.; Dapprich, S.; Daniels, A.D.; Farkas, Ö.; Foresman, J.B.; Ortiz, J.V.; Cioslowski, J.; Fox, D.J. *Gaussian 09*, **2009** Revision A.1, Gaussian, Inc., Wallingford CT.
11. Feller, S.E.; Gawrisch, K.; MacKerell, Jr., A.D. *J. Am. Chem. Soc.* **2002,** *124(2)*, 318–326.
12. Widrig, C.A., Alves, C.A., Porter, M.D., *J. Am. Chem. Soc.* **1991,** *113(8)*, 2805–2810.
13. Humphrey, W.; Dalke, A.; Schulten, K.; *J. Mol. Graphics* **1996,** *14*, 33–38.
14. Phillips, J.C.; Braun, R.; Wang, W.; Gumbart, J.; Tajkhorshid, E.; Villa, E.; Chipot, C.; Skeel, R.D.; Kale´, L.; Schulten, K. *J. Comput. Chem.* **2005,** *26(16)*, 1781–1802.
15. Jorgensen, W.L.; Chandrasekhar, J.; Madura, J.D.; Impey, R.W.; Klein, M.L. *J. Chem. Phys.* **1983,** *79(2)*, 926–935.
16. van Gunsteren, W. F. and Berendsen, H. J. C. *Mol. Phy.* **1977,** *34(5)*, 1311–1327.
17. Darden, T.; York, D.; Pedersen, L. *Chem. Phys.* **1993,** *98(12)*, 10089–10092.

Table S1: CHARMM Charges of MBN

```
RESI CBN        0.00
GROUP
ATOM N          NH1     -0.47           !    |                          HZ1  HN1
ATOM HN         H        0.31           !  HN-N                          |      |
ATOM CA         CT1      0.07           !    |    HB1                  CZ1--CN1
ATOM HA         HB       0.09           !    |     |                   //          \\
GROUP                                   !  HA-CA--CB--SG--SD--CE           CT--CI=-NK
ATOM CB         CT2     -0.10           !    |     |                    \    __     /
ATOM HB1        HA       0.09           !    |    HB2                   CZ2--CN2
ATOM HB2        HA       0.09           !   O=C                         |      |
ATOM SG         S       -0.08           !    |                          HZ2  HN2
GROUP
ATOM SD         S       -0.08
ATOM CE         CA       0.289
ATOM CZ1        CA      -0.115
ATOM HZ1        HP       0.115
ATOM CZ2        CA      -0.115
ATOM HZ2        HP       0.115
ATOM CN1        CA      -0.115
ATOM HN1        HP       0.115
ATOM CN2        CA      -0.115
ATOM HN2        HP       0.115
ATOM CT         CA      -0.029
ATOM CI         CNI      0.254
ATOM NK         NNI     -0.434
GROUP
ATOM C          C        0.51
ATOM O          O       -0.51
```

Table S2: Structural parameters of MBN-labelled K8C and MBN-labelled K39C on the SAM coated gold layer.

	MBN-labelled K8C	MBN-labelled K39C
Distance (-CN – gold) / Å	22.1	44.8
Angle (heme – surface normal) / degrees	104.9	127.3
Angle (-CN – heme) / degrees	121.2	93.8

Figure S1: Analysis of the IR and SEIRA spectra of MBN-labelled Cyt-c.

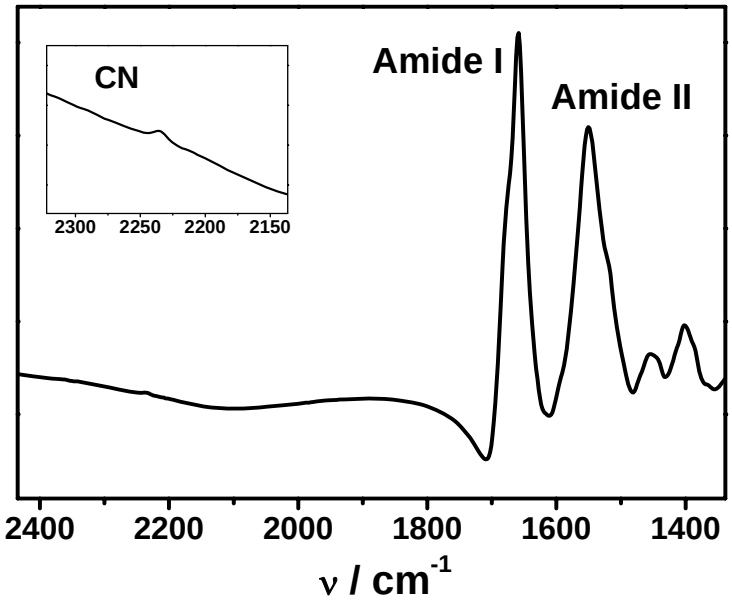

Left: Absolute SEIRA spectrum of MBN-labelled K39C Cyt-c; the inset displays the CN stretching region in an expanded view.

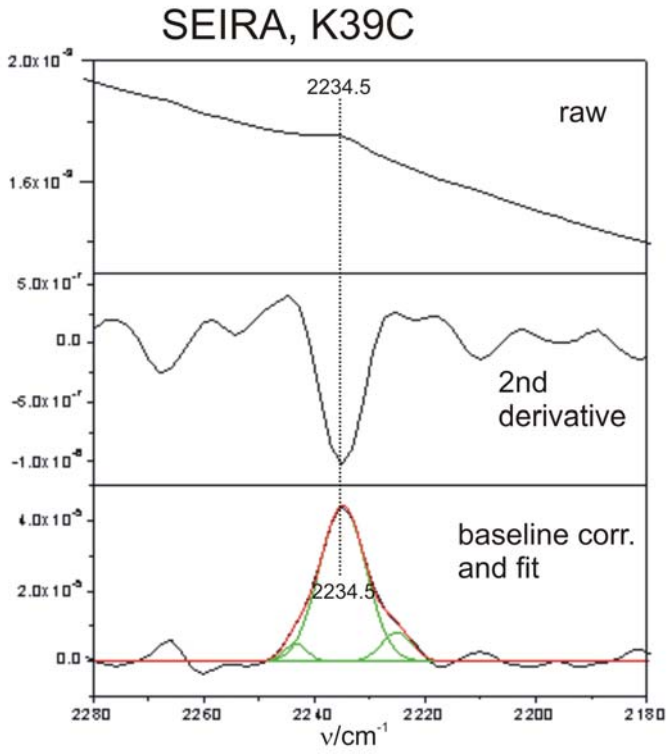

Spectra analysis demonstrated for a SEIRA measurement of the K39C labelled protein. Top: absolute spectrum, middle: 2nd derivative, bottom: spectrum after baseline subtraction, including a multi-Gaussian fit

Figure S2: a) Cyclic voltammogram of MBN-labelled K39C Cyt-c recorded at a scan rate of 50 mV/sec while in the SEIRA setup. b) Redox-induced SEIRA difference spectra of MBN-labelled K39C Cyt-c measured as described previously.[6]

The redox potentials determined by CV are, within the error margin, the same as that measured for the wild-type protein (i.e. 0.02 V).[6] The potential-dependent SEIRA difference spectra demonstrate the structural integrity of the immobilised variant proteins, although the redox potentials derived from these spectra are slightly more positive.

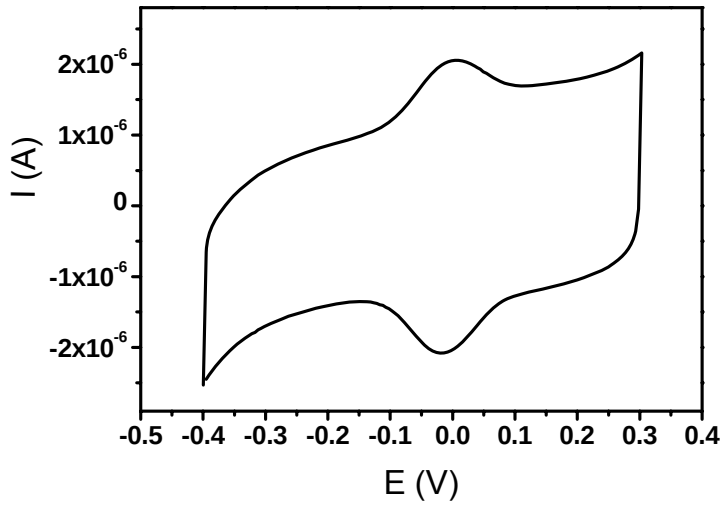

a

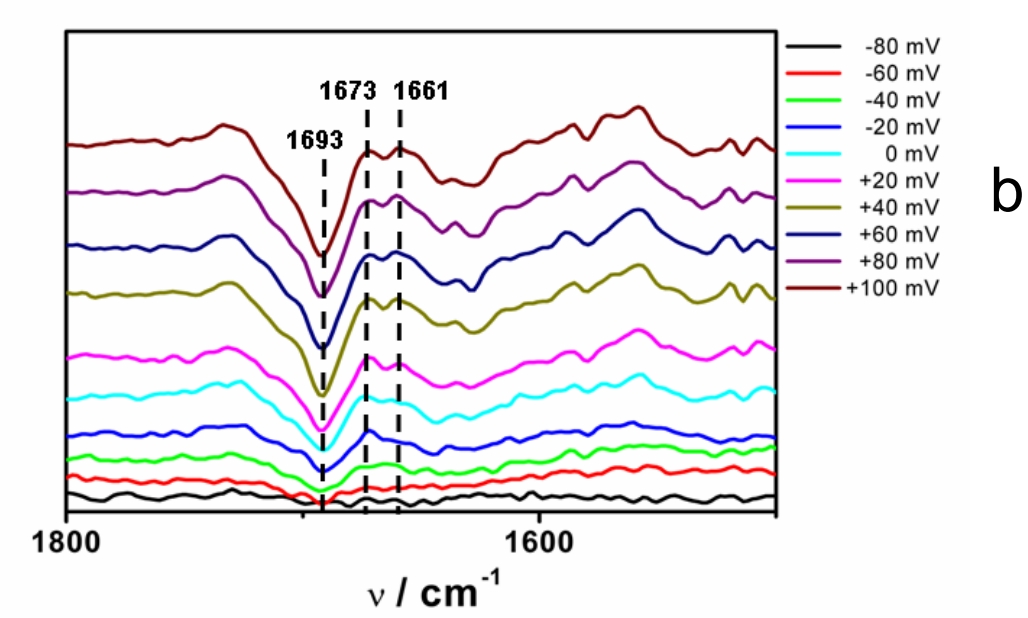

b

Figure S3: FT-Raman spectra recorded for solid MBN and for MBN dissolved in DMSO.

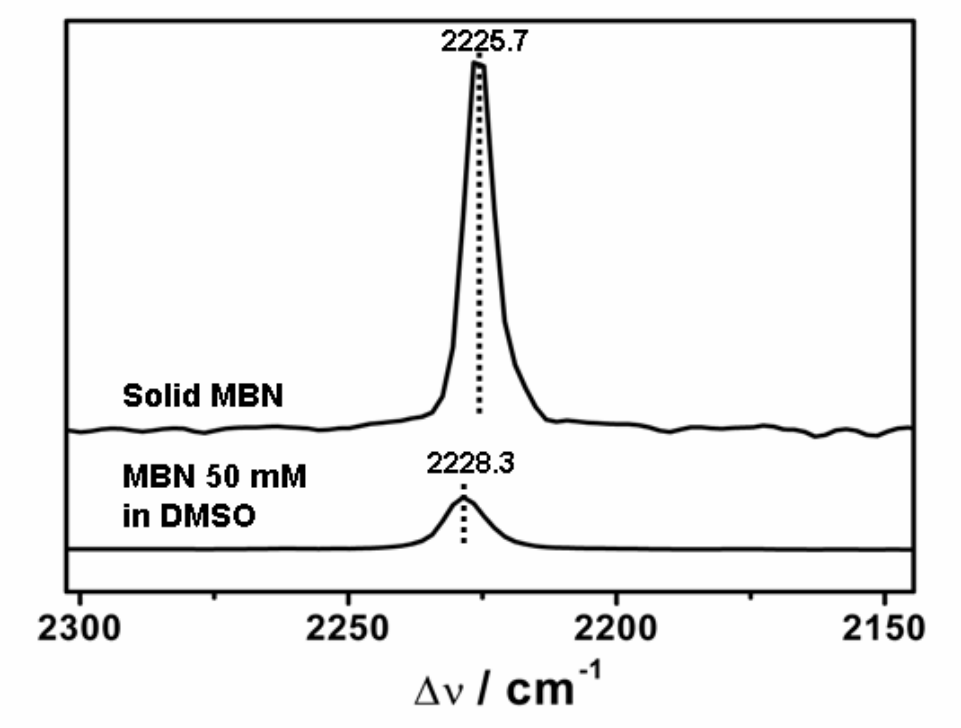

Figure S4: Total energy during MD: a) MBN labelled K8C (solution), b. MBN labelled K39C (solution), c. MBN labelled K8C (surface), d. MBN labelled K39C (surface). ((c and d on the following page)

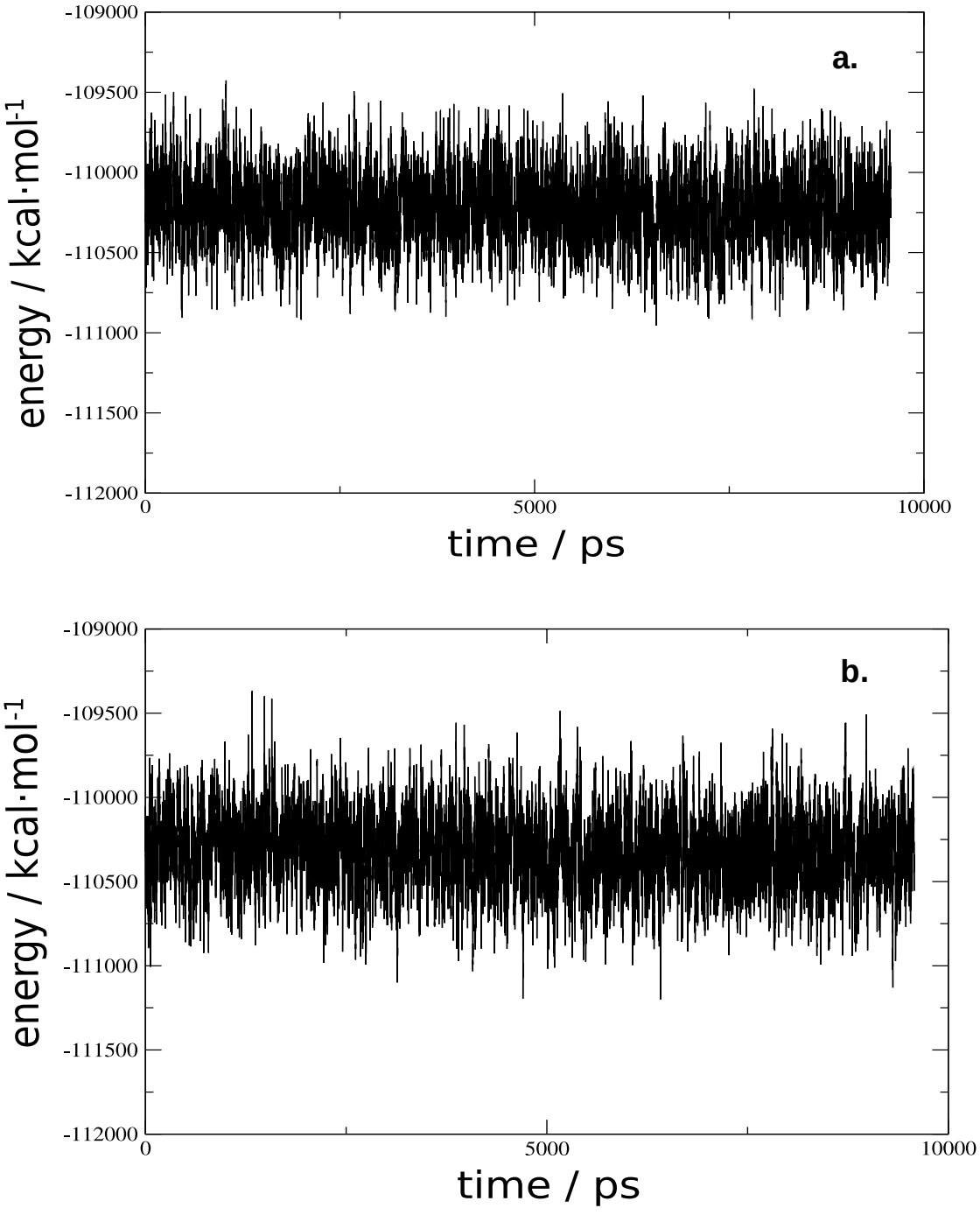

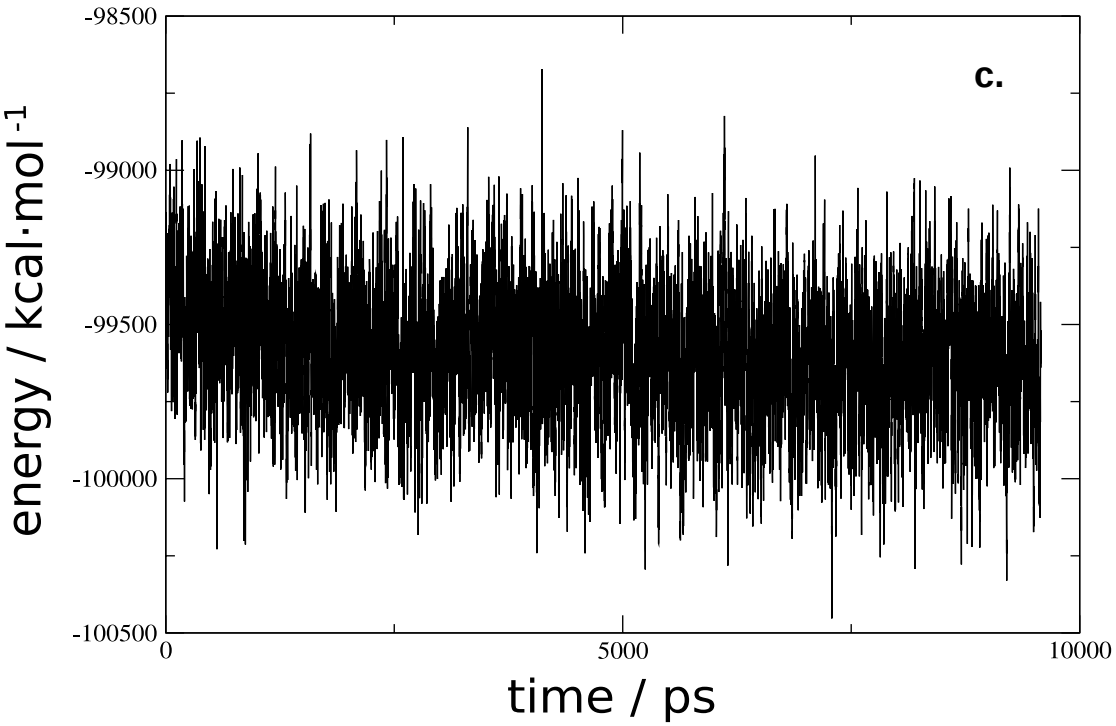

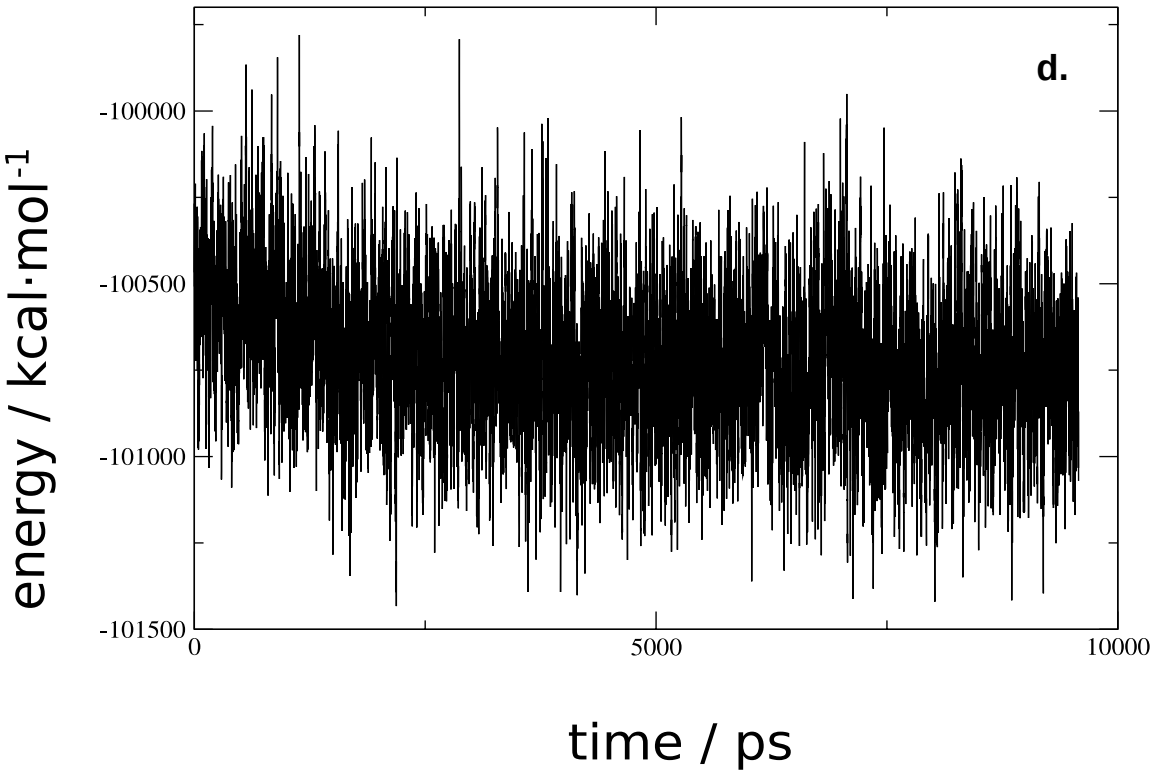

Figure S5: RMSD of the protein backbone during MD: a) MBN labelled K8C (solution), b) MBN labelled K39C (solution), c) MBN labelled K8C (surface), d) MBN labelled K39C (surface) (c and d on the following page)

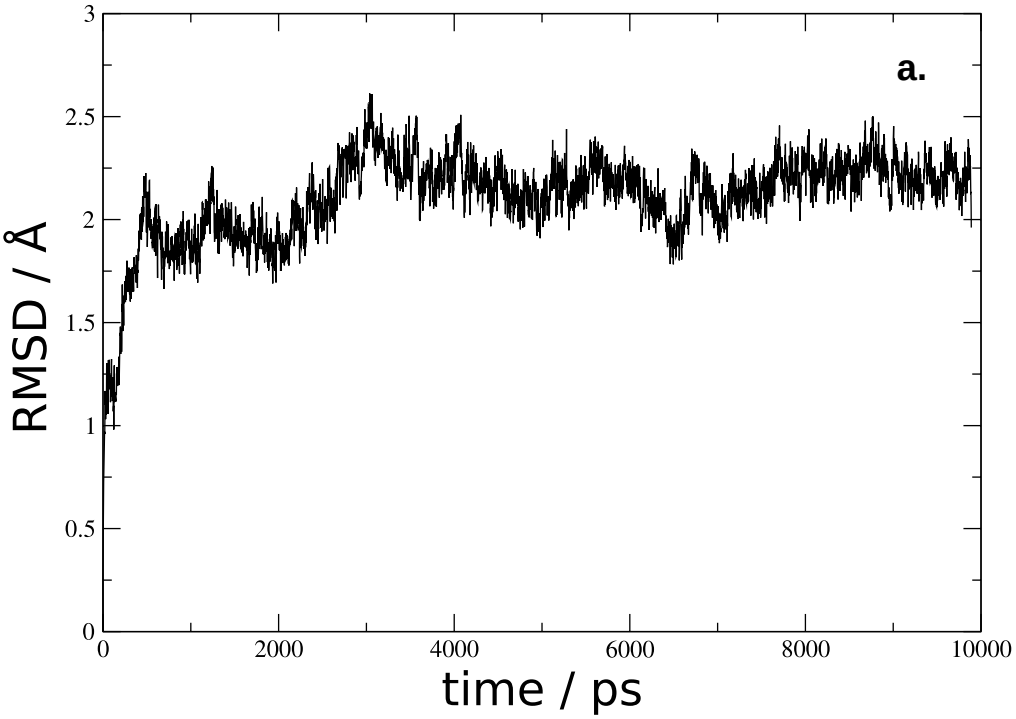

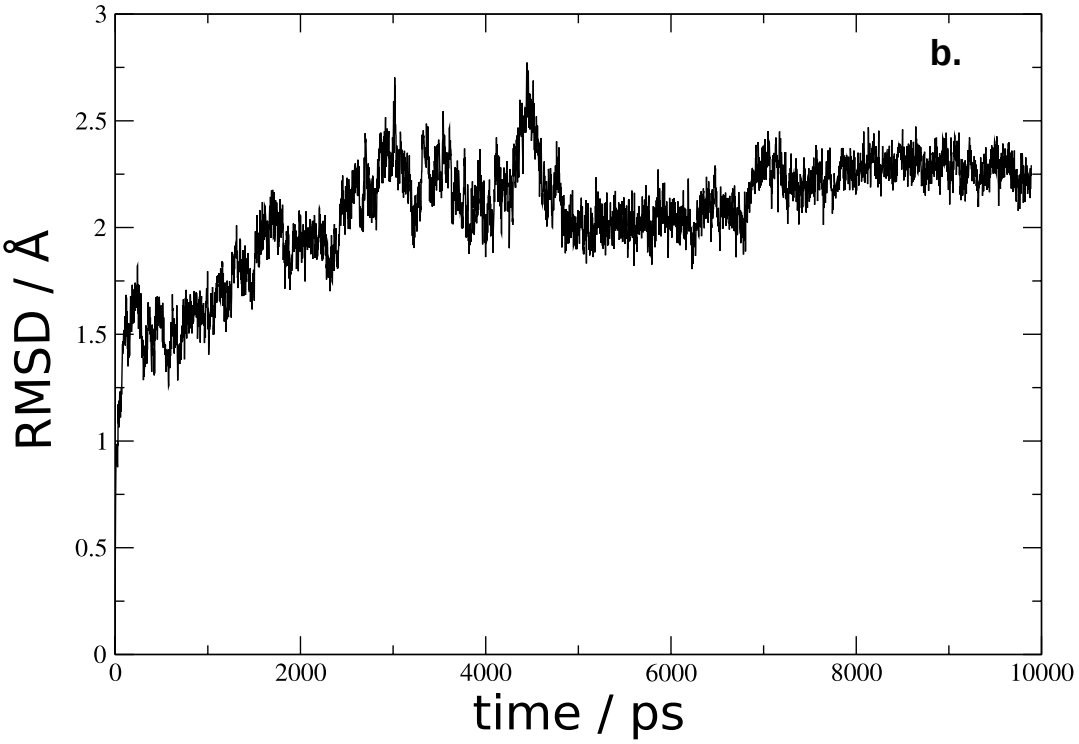

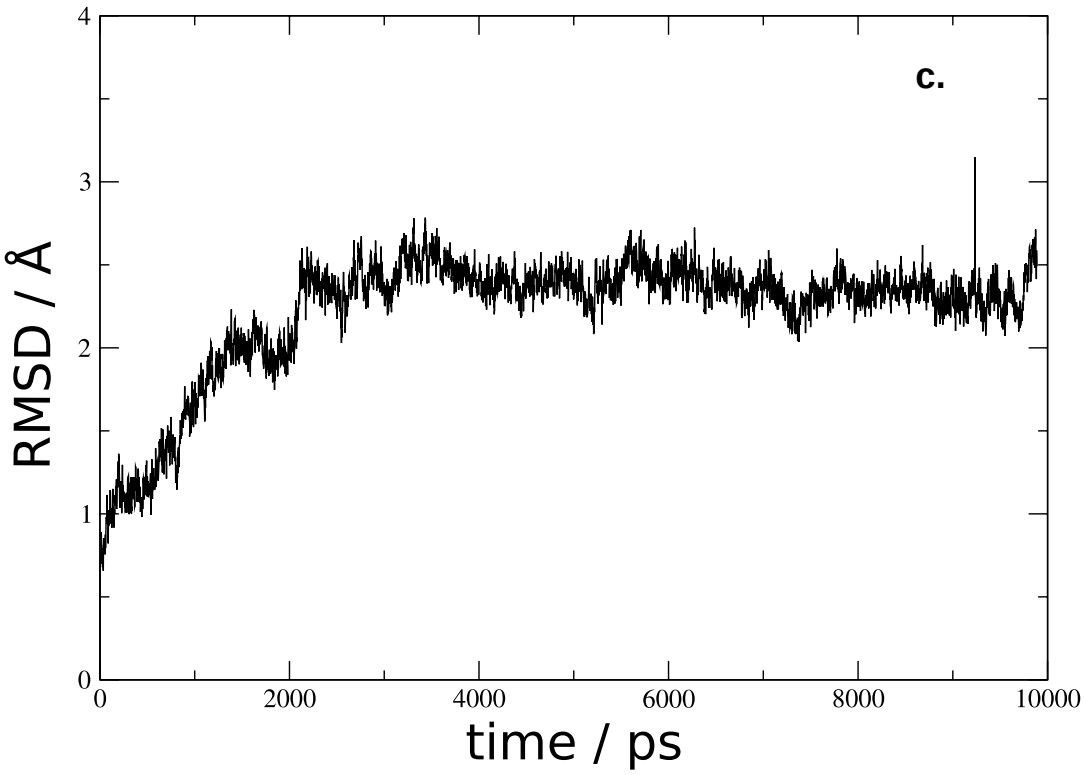

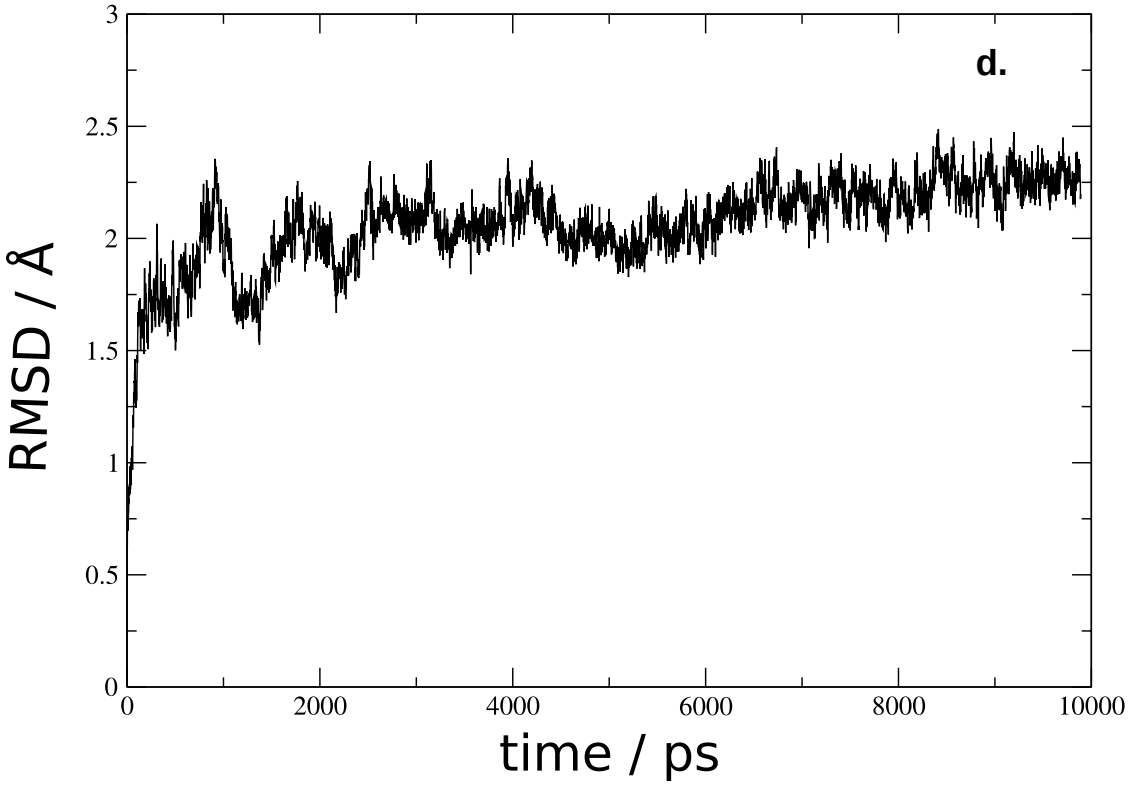

Figure S6: Changes of the angle between the CN bond and the surface normal during MD (5 – 10 ns): a) MBN labelled K8C (surface), b) MBN labelled K39C (surface), the red line indicates the average value.

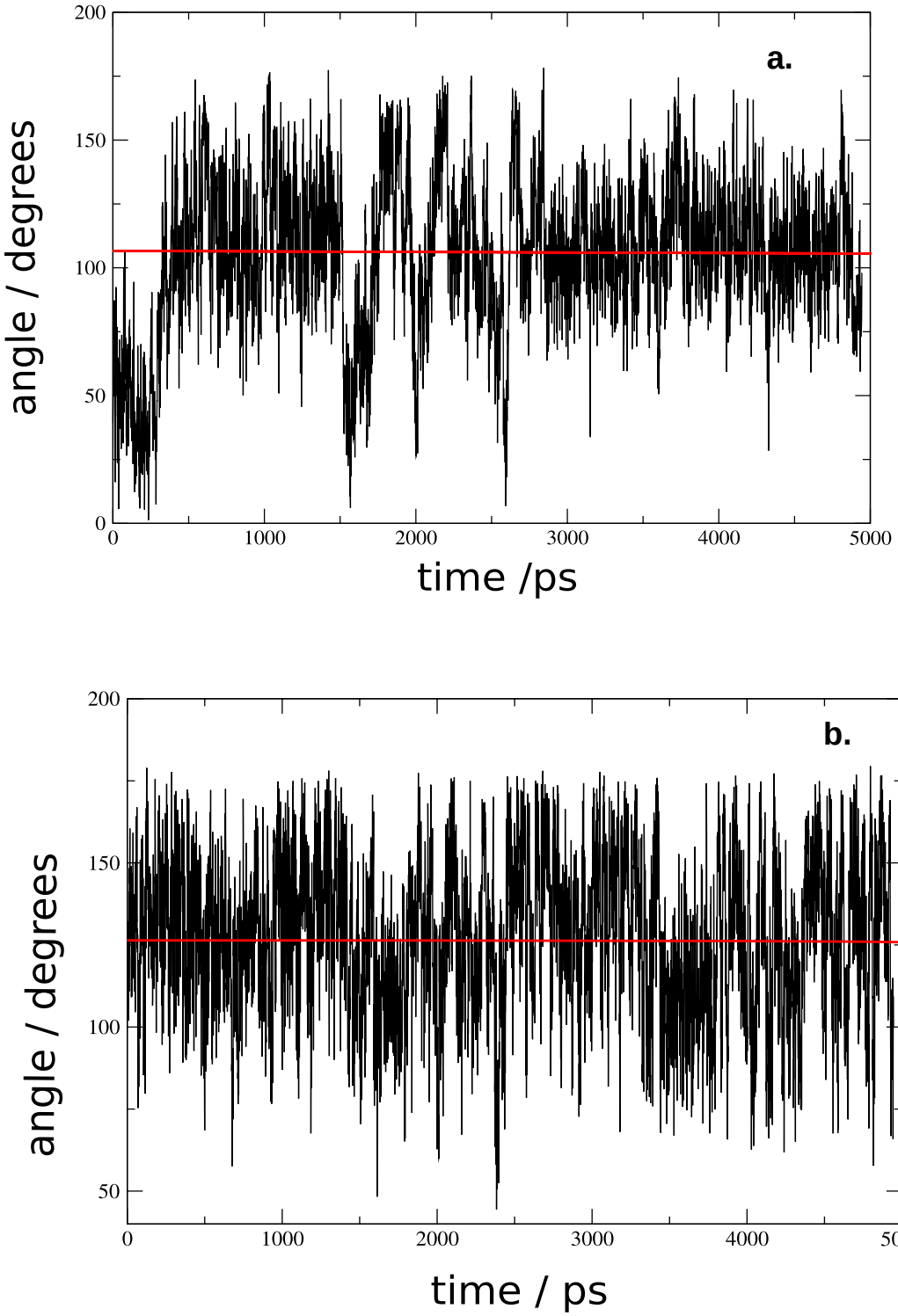

Figure S7: Distances between the center of the CN bond and gold surface during MD (5 – 10 ns): a) MBN labelled K8C (surface), b) MBN labelled K3C (surface), the red line indicates the average values.

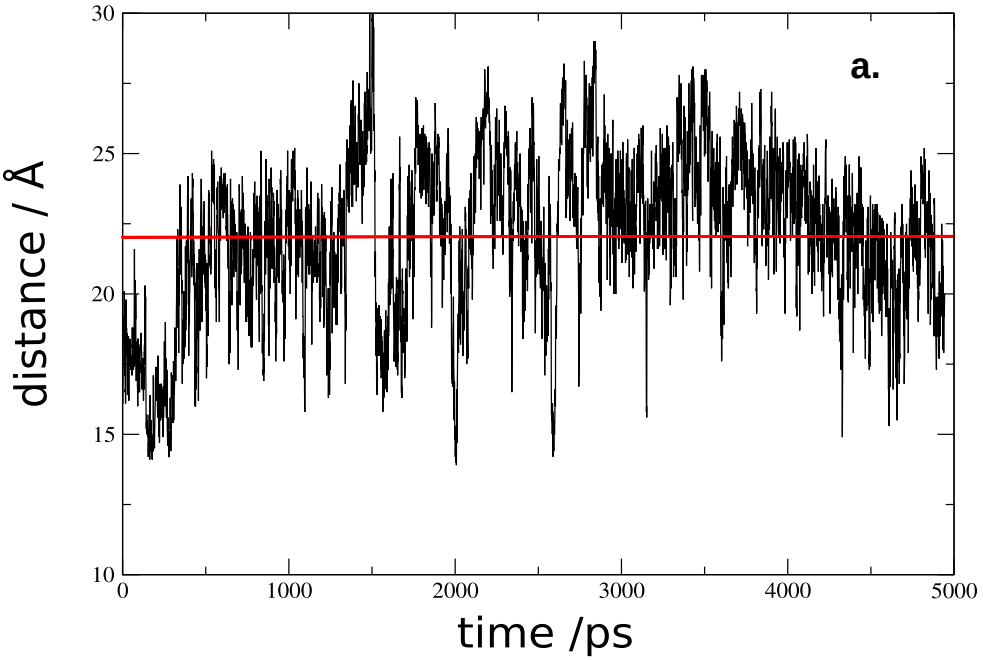

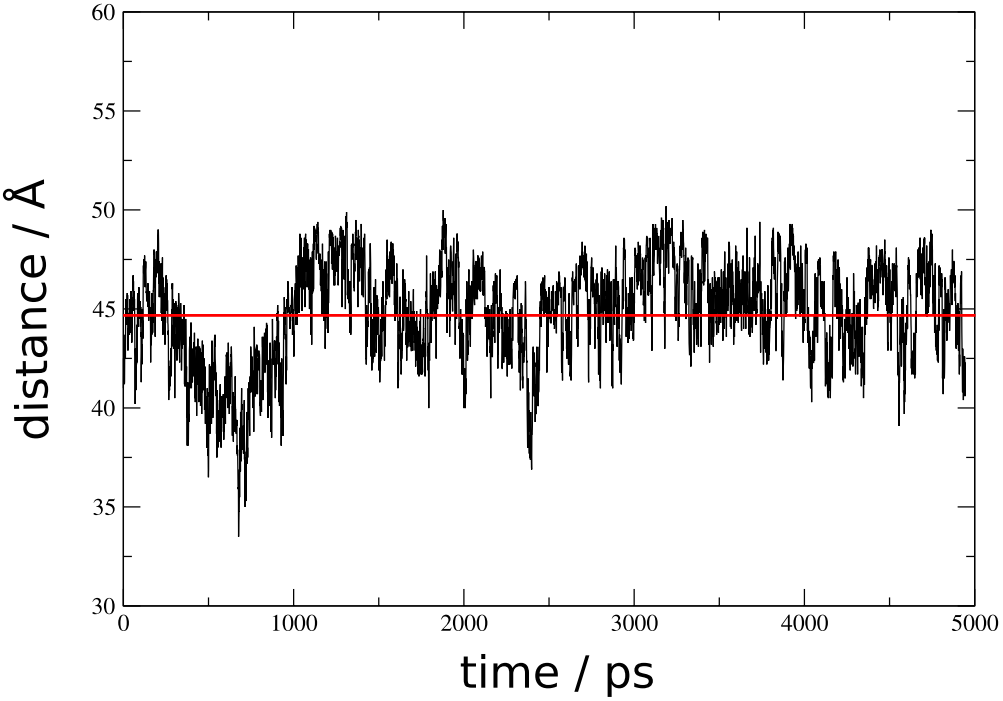

Figure S8: Number of contacts of the nitrile label (N atom) of K8C (black) and K39C (red) with solvent water molecules during the MD simulations. In solution (top figures), the average numbers of contacts are 3.37 and 3.63 for the nitrile labels of K8C and K39C, respectively. Essentially the same values were obtained for the immobilised protein (bottom figures, 3.44 for K8C and 3.62 for K39C).